



This article appeared in a journal published by Elsevier. The attached copy is furnished to the author for internal non-commercial research and education use, including for instruction at the authors institution and sharing with colleagues.

Other uses, including reproduction and distribution, or selling or licensing copies, or posting to personal, institutional or third party websites are prohibited.

In most cases authors are permitted to post their version of the article (e.g. in Word or Tex form) to their personal website or institutional repository. Authors requiring further information regarding Elsevier's archiving and manuscript policies are encouraged to visit:

<http://www.elsevier.com/copyright>

Contents lists available at [SciVerse ScienceDirect](http://www.sciencedirect.com)

## Continental Shelf Research

journal homepage: [www.elsevier.com/locate/csr](http://www.elsevier.com/locate/csr)

## Research papers

## Evidence of a recent rapid subsidence in the S–E Cyclades (Greece): An effect of the 1956 Amorgos earthquake?

N. Evelpidou<sup>a,\*</sup>, D. Melini<sup>b</sup>, P. Pirazzoli<sup>c</sup>, A. Vassilopoulos<sup>d</sup><sup>a</sup> *Faculty of Geology and Geoenvironment, National and Kapodistrian University of Athens, Greece*<sup>b</sup> *Istituto Nazionale di Geofisica e Vulcanologia, Roma, Italy*<sup>c</sup> *CNRS-Laboratoire de Géographie Physique, Meudon, France*<sup>d</sup> *Geoenvironmental Institute, Naxos 2-4, Doukissis Plakentias, Chalandri, 15238, Athens, Greece*

## ARTICLE INFO

## Article history:

Received 8 May 2011

Received in revised form

5 March 2012

Accepted 23 March 2012

Available online 30 March 2012

## Keywords:

Co-seismic

Post-seismic effect

Tidal notch

Sea-level change

Crustal thinning

Extensional tectonic regime

## ABSTRACT

An underwater geomorphological survey along the coasts of six Cycladic islands (Sifnos, Antiparos, Paros, Naxos, Iraklia and Keros) revealed widespread evidence of a recent 30–40 cm submergence, part of which may have seismic origin. Comparison with information reported from earthquakes having affected the area suggests that at least part of the recent submergence might be an effect of the 1956 Amorgos earthquake. Modelling of the co-seismic and short-term post-seismic effects of the earthquake revealed that part of the observed subsidence may be explained in some of the islands by a fast post-seismic relaxation of a low-viscosity layer underlying the seismogenic zone. However far-field observations are underestimated by our model, and may be affected by a wider deformation field induced by the largest aftershock of the Amorgos sequence, or by other earthquakes.

© 2012 Elsevier Ltd. All rights reserved.

## 1. Introduction

In the midlittoral zone, very narrow in the Mediterranean, parallel vegetational belts are more developed. Eroding Cyanobacteria, patellaceous gastropods (limpets) and chitons are more abundant (Laborel and Laborel-Deguen, 2005). They all contribute, by eating the vegetational belts, to the erosion of the underlying rock and enable the development (in sites sheltered from strong wave action) of a reclined U-shaped or V-shaped intertidal notch, with a vertex located near MSL, the base near the lowest tide level and the top near the highest tide level (Pirazzoli, 1986). The profile of a tidal notch is an excellent sea-level indicator, because it provides information on the duration in which MSL remained at the level of the notch vertex and, if the notch is emerged or submerged, on the speed (slow or even sudden) of its emergence or submergence (Pirazzoli, 2005). If notch profiles cannot testify of transient sea-level changes of meteorological origin, like tide-gauge records or the measurement of a biological datum (Stiros and Pirazzoli, 2004), they can be most useful for longer-term or even sudden relative sea-level variations. In addition, notch profiles can be modified by

sufficiently long enduring changes in the relative sea level, thus testifying of pre-seismic or post-seismic gradual tectonic trends. However, when certain subsidence displacements add to a sea-level rise trend of eustatic origin greater than the possibilities of bioerosion, like the elevation changes measured during the interval 1969–1984 across the Atalandi Fault–Zone (Stiros and Rondogianni, 1985), they contribute to the absence of a present-day tidal notch development (Evelpidou et al., 2011a).

Carbonate rocks are generally favourable to the development and preservation of tidal notches, while gneisses, schists, amphibolites, terrestrial deposits and volcanic rocks are less affected by bioerosion. The most favourable conditions for notch formation occur where the cliff is vertical, while the slope of the cliff or irregularities in the rock surface may retard or even prevent the development of a clear notch profile.

In the case of gradual relative sea-level rise, calculations show that the inward depth of a tidal notch remains very limited, while its height tends to increase. Beyond certain subsidence rates, the possibilities of notch development may even disappear.

Many examples on the value of notches for coastal tectonics have been provided, especially in the Eastern Mediterranean (e.g., Pirazzoli, 1980, 2005; Pirazzoli et al., 1991; Stiros et al., 2000, 2009; Morhange et al., 2006; Evelpidou et al., 2011b).

The study area is situated in the central Cycladic islands, located in the central Aegean Sea (Greece) (Fig. 1). The geology of the area consists mainly of metamorphic rocks such as mica

\* Corresponding author.

E-mail addresses: [evelpidou@geol.uoa.gr](mailto:evelpidou@geol.uoa.gr) (N. Evelpidou), [daniele.melini@ingv.it](mailto:daniele.melini@ingv.it) (D. Melini), [paolop@noos.fr](mailto:paolop@noos.fr) (P. Pirazzoli), [vassilopoulos@geoenvi.org](mailto:vassilopoulos@geoenvi.org) (A. Vassilopoulos).

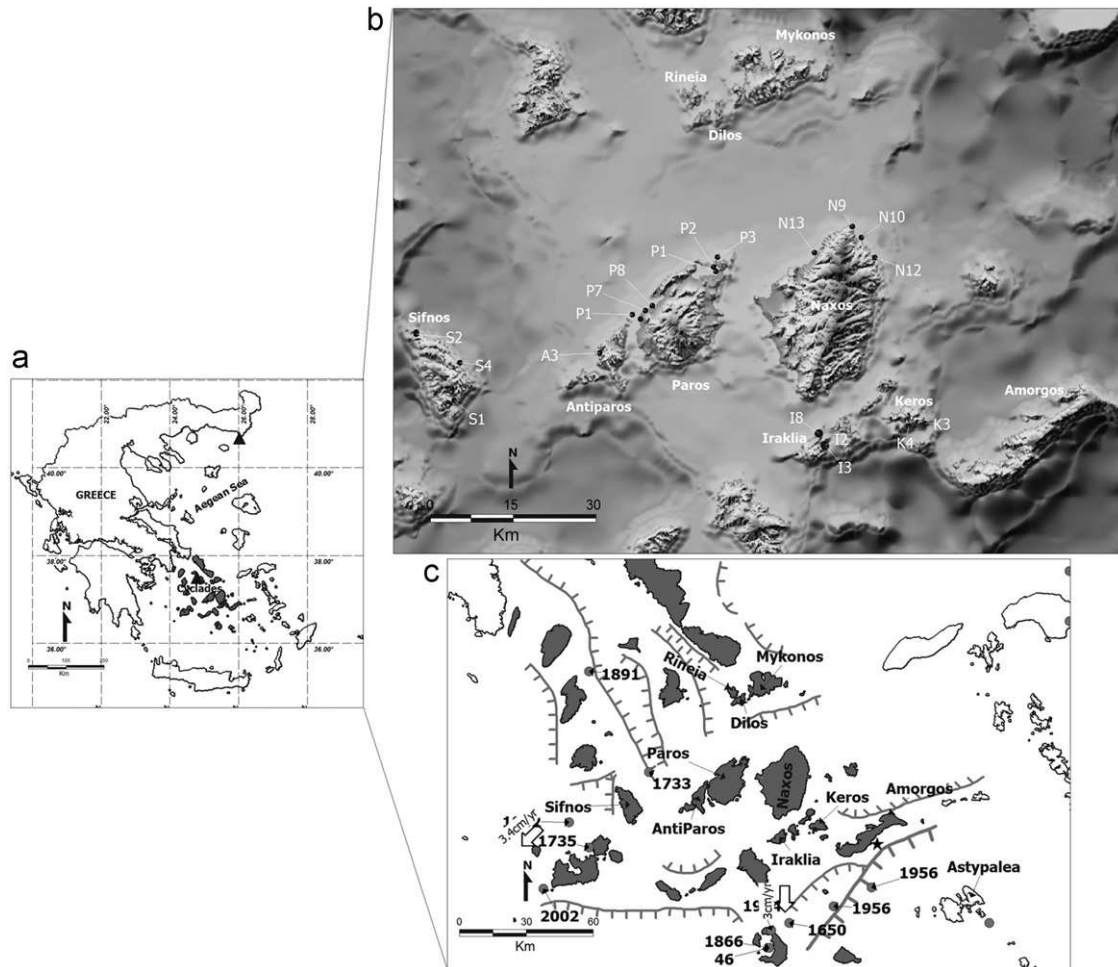


**Fig. 1.** (a) Studied area. Triangles show the tide gauges at Alexandroupolis (northern Greece) and Syros (Cyclades) (b). Sites discussed in the text and in Table 1(c). Main active faults in Cyclades and the rates and direction of motion of Cyclades during Quaternary – A.A.T. – Amorgos–Astypalea trough. The offshore faultlines that seems to coincide with the surface rupture of the 1956 earthquake (Papadopoulos and Pavlidis, 1992; Stiros et al., 1994) is marked with a heavier line. Asterisk at Amorgos island depicts Aghia Anna beach, where a 40 cm uplifted bench has been identified by Stiros et al. (1994). The historical earthquakes with  $M_s > 6$  having occurred in the wider studied area are also depicted.

schists, marbles, gneisses, amphibolites, glaucophane schists and plutonic rocks (Papanikolaou et al., 1981; Papanikolaou, 1987).

In the surveyed area, we observed that a tidal notch was generally absent from the present midlittoral zone, but there was, most often, a submerged notch present a few decimetres below sea level.

After a description of the observed geomorphological remains of submerged tidal notches, we shall discuss their implication for the interpretation of the recent tectonic history in the area and the possibility that at least part of the observed recent submergence is a consequence of one of the earthquakes that affected the area during the last century.

In the present paper we present new results confirming the occurrence of a recent period of some centuries relative sea-level stability, followed by a recent submergence of 30–40 cm, possibly in part of seismic origin, that affected several Cycladic islands at about the same time.

## 2. The geodynamic context

The study area is presumably under an extensional tectonic regime behind the modern volcanic arc at the centre of the Aegean plate and possesses a relatively thin continental crust of about 28–30 km. This is owed to two factors, the gravitational

collapse of the Aegean crust due to the southward retreat of subduction front during the Cenozoic and the westwards extrusion of the Anatolian block in the Aegean during the Neogene (Tirel et al., 2004). The general trend of the major submarine fault tectonism is from east to west, exhibiting a curved shape and coinciding with the volcanic and back arc Cycladic area. In recent years, several major offshore faults have been identified suggesting the presence of tectonic depressions with horsts (Lykousis et al., 1995; Doutsos and Kokkalas, 2001; Evelpidou, 2001; Tirel et al., 2004).

It is generally accepted that the tectonic regime affecting the Aegean is broadly extensional (e.g., McKenzie, 1978; Mercier et al., 1989; Papazachos, 1990), and dominated by normal faulting. Main active faults of the studied area are depicted in Fig. 1.

The Aegean Region is characterised by intense seismic activity due to the rapidly deforming broader Eastern Mediterranean area and its complex neotectonic structure (Pavlidis and Caputo, 2004). Although the Aegean Region has one of the longest and densest records of historical seismicity in the world (e.g., Galanopoulos, 1981; Guidoboni et al., 1994; Papazachos and Papazachou, 1997; Pavlidis, 1996a), available knowledge about co-seismic surface ruptures in the region is very limited (Ambraseys and Jackson, 1990; Pavlidis et al., 2000; Goldsworthy et al., 2002). The historical database for the study area is incomplete, (Pavlidis and Caputo, 2004) and our knowledge of the offshore active faults

of the Aegean Region is extremely limited because many of the epicentres are located submarine.

Instrumental data cover less than 100 years and the historical information can be considered relatively complete from the 19th century onwards. Where earthquake repeat times are less than 100 or 200 years such information might be adequate. However, palaeoseismological researches in Greece have shown that the average recurrence interval of specific active faults is commonly longer than 500 years and usually some thousands years (Pavlidis, 1996b; Pantosti et al., 1996; Chatzipetros et al., 1998; Caputo et al., 1998). This means that several other earthquakes may have occurred in the area but may have not been recorded. For instance, in the nearby island of Kea, archaeological data testify an earthquake which produced characteristic destruction in prehistoric buildings, coastal subsidence and contamination of a near-coastal source by saline water, which caused abandonment of the site (Stiros, 2005).

The high seismicity is of intermediate depth in the South Aegean and shallow almost everywhere else in the Aegean and adjacent regions. However, part of the central and South Aegean has been recognised as an "aseismic plateau" (e.g., Morelli et al., 1975).

The Amorgos Island earthquake of 9th July, 1956 that took place on the eastern boundary of this plateau is the largest ( $M_s=7.4$ ) crustal event taken place this century in Greece and clearly indicates that the Aegean is affected by strong earthquakes but with longer recurrence intervals than in adjacent areas.

The active SSW–NNE trending subduction beneath the South Aegean is believed to be the main cause of many geophysical phenomena in the Aegean (e.g., Papazachos and Papadopoulos, 1977; McKenzie, 1978).

According to Lykousis (2009), a continuous and gradual subsidence predominated during the last 400 ka, with values of 0.34–0.60 mm/yr for the Cycladic plateau, with a gradual decrease in the intensity of the extensional tectonic regime. The relative motion of the Cyclades during the Quaternary is towards the south and south-west with a rate of about 3 cm/yr (Peterek and Schwarze, 2004).

The crust in the Cycladic area is rather thinner than normal. The Cycladic plateau, which is generally less than 200 m deep, lies mostly underwater because of the thinner crust. The thinning is a result of the widespread Neogene and Quaternary spreading of the crust of this area, as well as the westward extrusion of the Anatolia block.

The subsidence during the late Holocene is confirmed by the frequent evidence of submerged coastal archaeological remains, like at Kea (Karthea–drowned quay), Tinos (Kionia–submerged walls) Kythnos and Naxos (Gaki-Papanastassiou et al., 2010). Flemming and Webb (1986) mention three submerged sites in Paros, one at a depth of –5 m having an age of 7000 years and two at depths of –3 m having an age of 2400 years.

Desruelles et al. (2009) have reported from the Mykonos–Delos–Rhenia area three levels of submerged beachrocks, at  $-3.6 \pm 0.5$  m from about 2000 BC, at  $-2.5 \pm 0.5$  m from 400 BC, and  $-1 \pm 0.5$  m from around 1000 AD. According to Desruelles et al. (2009), beachrock formation requires vertical stability of the shoreline during a certain time.

### 3. Methods

Detailed, accurate and systematic survey along the coastal zone of Sifnos, Antiparos, Paros, Naxos, Iraklia and Keros took place during spring and summer 2010. The coasts of the study area (Fig. 1) were systematically surveyed in detail, by a boat in order to access all sites and to establish their continuity.

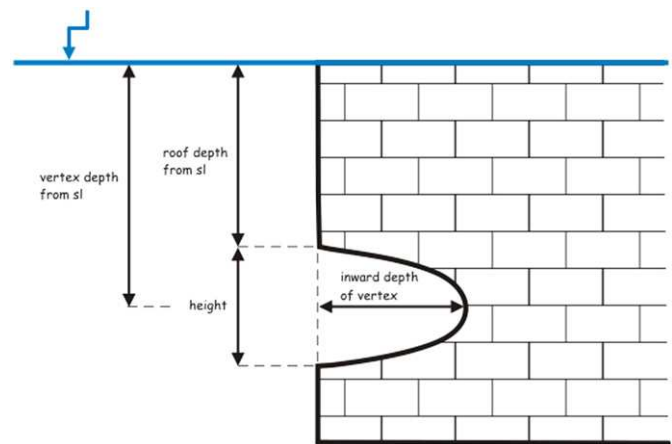


Fig. 2. Schema depicting measurement points on a notch.

Due to the complete absence of elevated shorelines and even to the lack of clear marks of a tidal notch in the present midlittoral zone, even in rock formations that could be expected favourable to its formation, our survey was extended underwater along the rock cliffs. Marks of submerged shorelines could be identified only when the rock was not too stratified and favourable to bioerosion. During the survey, the local lithology of the Cyclades was taken into account.

Forty-three immersions were made along the study area in the Cyclades (four in Koufonissia–Keros, eight in Iraklia, eight in Paros, four in Antiparos, thirteen in Naxos and six in Sifnos).

Former shorelines were identified from submerged notches. For each immersion, the time and the GPS geographical coordinates were collected (with an average accuracy of  $\pm 5$  cm) and, underwater, the observed features were measured in relation to sea level at the time of observation (with an accuracy that, due to waves, may be estimated at about  $\pm 10$  cm) and photographed. Notch geometries (e.g., retreat point elevation and height) were measured according to Pirazzoli (1986) (Fig. 2). Several measurements were performed on each location and the accuracy was improved by multiple measurements. Comparisons were made in Table 1 with six-hourly records of pressure at sea level at Naxos, (downloaded from the archive of the Russian meteorological site (<http://meteo.infospace.ru/wcarch/html>) and with hourly tidal records at Syros (provided by the Hellenic Hydrographic Service) with the aim not to improve the accuracy of measurements, that can hardly decrease below about  $\pm 10$  cm, but to confirm in certain cases the validity of the interpretation (see below). Although more than one submerged shoreline could be observed and measured at certain sites, the present work is devoted to the distribution and size of the upper submerged shoreline, which is summarised in Table 1 and, for some significant photographs, in Fig. 3.

### 4. Results of observations

The almost complete absence of tidal notch development in the present intertidal range is noticed in all surveyed islands. The roof depth of the upper submerged notch is most often about two decimetres below sea level at the time of measurement, with some values however slightly greater at Iraklia and even no apparent submergence at some sites of Naxos (Table 1). At Sites 9, 10 and 12 of Naxos, in particular, the notch could, at first view, be interpreted as a present-day tidal notch at high tide. However this possibility could be discarded after analysis of air pressure records (that were slightly higher than normal, thus implying

**Table 1**  
Size of the submerged notch profiles in the southeastern Cyclades.

| Island              | Site N°<br>(Fig. 1) | Long. E      | Lat. N       | Time (yymmdd)<br>and air pressure<br>(P0) at Naxos | Notch measurement (cm)   |                            |                              |        | Genesis<br>(Fig. 4) | Illustration<br>(Fig. 3) |
|---------------------|---------------------|--------------|--------------|--|--------------------------|----------------------------|------------------------------|--------|---------------------|--------------------------|
|                     |                     |              |              |  | Roof<br>depth<br>from SL | Vertex<br>depth<br>from SL | Inward<br>depth<br>of vertex | Height |                     |                          |
| Sifnos              | S1                  | 24°44'25.61" | 36°55'25.59" | 100,814–1,012                                      | 22                       | 36                         | 20                           | 28     | a'                  | a                        |
|                     | S2                  | 24°38'49.96" | 37°2'7.32"   | 100,814–1,012                                      | 26                       | 37                         | 20                           | 22     | a'                  |                          |
|                     | S4                  | 24°44'10.40" | 36°59'5.43"  | 100,817–1,009                                      | 22                       | 37                         | 10                           | 30     | a'                  |                          |
| Antiparos           | A1                  | 25°5'20.43"  | 37°3'40.01"  | 100,805–1,005                                      | 20                       | 32                         | 15                           | 25     | a'                  | d                        |
|                     | A3                  | 25°1'16.45"  | 36°59'56.08" | 100,804–1,003                                      | 20                       | 37                         | 13                           | 34     | a'                  |                          |
| Paros               | P1                  | 25°15'38.38" | 37°7'46.22"  | 100,806–1,010                                      | 20                       | 36                         | 20                           | 32     | b'                  | c                        |
|                     | P2                  | 25°15'20.28" | 37°8'12.83"  | 100,806–1,010                                      | 20                       | 40                         | 28                           | 41     | b'                  |                          |
|                     | P3                  | 25°15'53.82" | 37°9'12.04"  | 100,806–1,010                                      | 20                       | 40                         | 22                           | 40     | b'                  |                          |
|                     | P6                  | 25°6'18.73"  | 37°3'12.6"   | 100,806–1,010                                      | 20                       | 30                         | 20                           | 20     | b'                  |                          |
|                     | P7                  | 25°6'57.38"  | 37°4'1.99"   | 100,806–1,010                                      | 20                       | 40                         | 22                           | 40     | c'                  |                          |
|                     | P8                  | 25°7'47.96"  | 37°4'30.42"  | 100,806–1,012                                      | 20                       | 41                         | 20                           | 43     | a'                  |                          |
| Naxos               | N9                  | 25°32'31.43" | 37°12'1.77"  | 100,425–1,015                                      | 0                        | 35                         | 24                           | 71     | b'                  | b                        |
|                     | N10                 | 25°33'33.43" | 37°10'54.11" | 100,425–1,015                                      | 0                        | 20                         | 32                           | 40     | b'                  |                          |
|                     | N12                 | 25°35'8.48"  | 37°8'55.59"  | 100,425–1,015                                      | 0                        | 30 (est.)                  | 15                           | nm     | b'                  |                          |
|                     | N13                 | 25°28'3.98"  | 37°9'21.99"  | 100,807–1,011                                      | 10                       | 42                         | 20                           | 65     | c'                  |                          |
| Iraklia             | I2                  | 25°28'43.21" | 36°50'34.26" | 100,804–1,003                                      | 20                       | 27                         | 5                            | 15     | b'                  | e                        |
|                     | I3                  | 25°28'47.18" | 36°50'27.99" | 100,804–1,003                                      | 25                       | 45                         | 14                           | 40     | b'                  |                          |
|                     | I8                  | 25°28'3.10"  | 36°51'42.03" | 100,804–1,003                                      | 20                       | 37                         | 20                           | 35     | b'                  |                          |
| Keros               | K3                  | 25°40'57.85" | 36°52'32.47" | 100,803–1,007                                      | 20                       | 42                         | 15                           | 45     | b'                  | f                        |
|                     | K4                  | 25°38'57.74" | 36°52'19.2"  | 100,803–1,007                                      | 20                       | 34                         | 15                           | 29     | b'                  |                          |
| Average values (cm) |                     | 17.3         | 35.9         | 18.5   | 36.6                     |                            |                              |        |                     |                          |

a temporary drop in sea-level) and by comparison with the tidal records.

The regular shape of the submerged notches suggests that the vertical displacement has been sufficiently rapid not to modify its profile. The depth of the vertex below present sea level (20–45 cm, with an average of 36 cm) has been, most often, between 30 and 40 cm in all the islands considered, where such erosion marks could be formed and preserved.

Previous studies from various parts of the world, summarised by Pirazzoli (1986, Table 1), have estimated that intertidal erosion rates on calcareous shores may vary between 0.2 and 5 mm/yr. These variable rates of biologic origin depend not only from the rock type, but also from the local climate and biological environment, and reach higher rates in tropical areas. If only the Mediterranean region is considered, measurements available indicate a possible variability between 0.2 and 1 mm/yr (Evelpidou et al., 2011a), assuming they are formed in a uniform lithological, biological and climatic condition among all islands.

At Sifnos Island, at Site S1 (Fig. 3(a)) a regular tidal notch with a vertex at  $-36 \pm 10$  cm is developed. The 20 cm inward depth of the notch profile suggests the occurrence of a relatively stable sea-level during a period between 2 centuries and a millennium, depending on the rate of bioerosion, to enable its full development. At Site S2 the status of the upper notch is similar to that at the preceding site. At Site S4, the upper notch has been recognised with a vertex at about  $-37 \pm 10$  cm but an inward depth of vertex of 10 cm, suggesting the occurrence of a relatively stable sea-level during a period of 1–5 centuries. All aforementioned notches in Sifnos island belong to a'-type (Evelpidou et al., 2011a) and suggests a rapid subsidence, greater than the tidal range, preceded by a relative sea-level stability (Fig. 4).

At Antiparos Island, at Site A1, the upper submerged notch could be recognised from about  $-20 \pm 10$  to  $-45 \pm 10$  cm. The inward depth of vertex of 15 cm, suggests the occurrence of a relatively stable sea-level during a period between 1.5 centuries and 7.5 centuries. At Site A3 (Fig. 3(d)), the roof of the upper notch

is marked at  $-20 \pm 10$  cm while the vertex at  $-37 \pm 10$  cm. The inward depth of vertex of 13 cm, would require a period of 1.3 centuries to 6.5 centuries to form with a relatively stable sea-level under assumed conditions. Both aforementioned sites of Antiparos Island belong to a'-type (Evelpidou et al., 2011a) and suggest a rapid subsidence, greater than the tidal range, preceded by a relative sea-level stability (Fig. 4).

At Paros Island, at Site P1, a very clear tidal upper notch can be observed. Its vertex is at  $36 \pm 10$  cm below sea-level and its inward depth is about 20 cm suggesting a relatively stable sea-level during a period from 2 centuries and 1 millennium. At Site P2, an upper continuous notch exists, with a vertex at  $40 \pm 10$  cm below sea-level. Its inward depth is 28 cm suggesting a relatively stable sea-level during a period of 2.8 centuries and 1.4 millennium. At Site P3 (Fig. 3(c)), between  $-20 \pm 10$  and  $-60 \pm 10$  cm a tidal notch exists, showing an inward depth of about 22 cm, which suggests a relative sea level stability lasting between 2 centuries and 11 centuries. At Site P6 a tidal submerged notch exists between about  $20 \pm 10$  and  $40 \pm 10$  cm below sea-level. The inward depth of vertex of 20 cm, suggests the occurrence of a relatively stable sea-level during a period of 2 centuries to 1 millennium. At Site P8 a tidal notch, submerged between about  $20 \pm 10$  and  $63 \pm 10$  cm below sea-level has an inward depth of vertex of 20 cm, suggesting the occurrence of a relatively stable sea-level during a period of 2 centuries to 1 millennium. The notch profiles of Sites P1, P2, P3, P6 belong to b'-type (Evelpidou et al., 2011a) (Fig. 4) suggesting a rapid subsidence, greater than the tidal range, that was preceded by a period of relative sea-level stability. At Site P7 a tidal notch, submerged between about  $20 \pm 10$  and  $60 \pm 10$  cm below sea-level, reveals an inward vertex depth of 22 cm, which suggests a relatively stable sea-level during a period of 2.2–11 centuries. The c'-type (Evelpidou et al., 2011a) (Fig. 4) suggests under the assumed conditions a rapid subsidence (smaller than the tidal range), preceded and followed by a relative sea-level stability, which produced a notch-profile considered in the new intertidal range and shifted the former notch underwater.

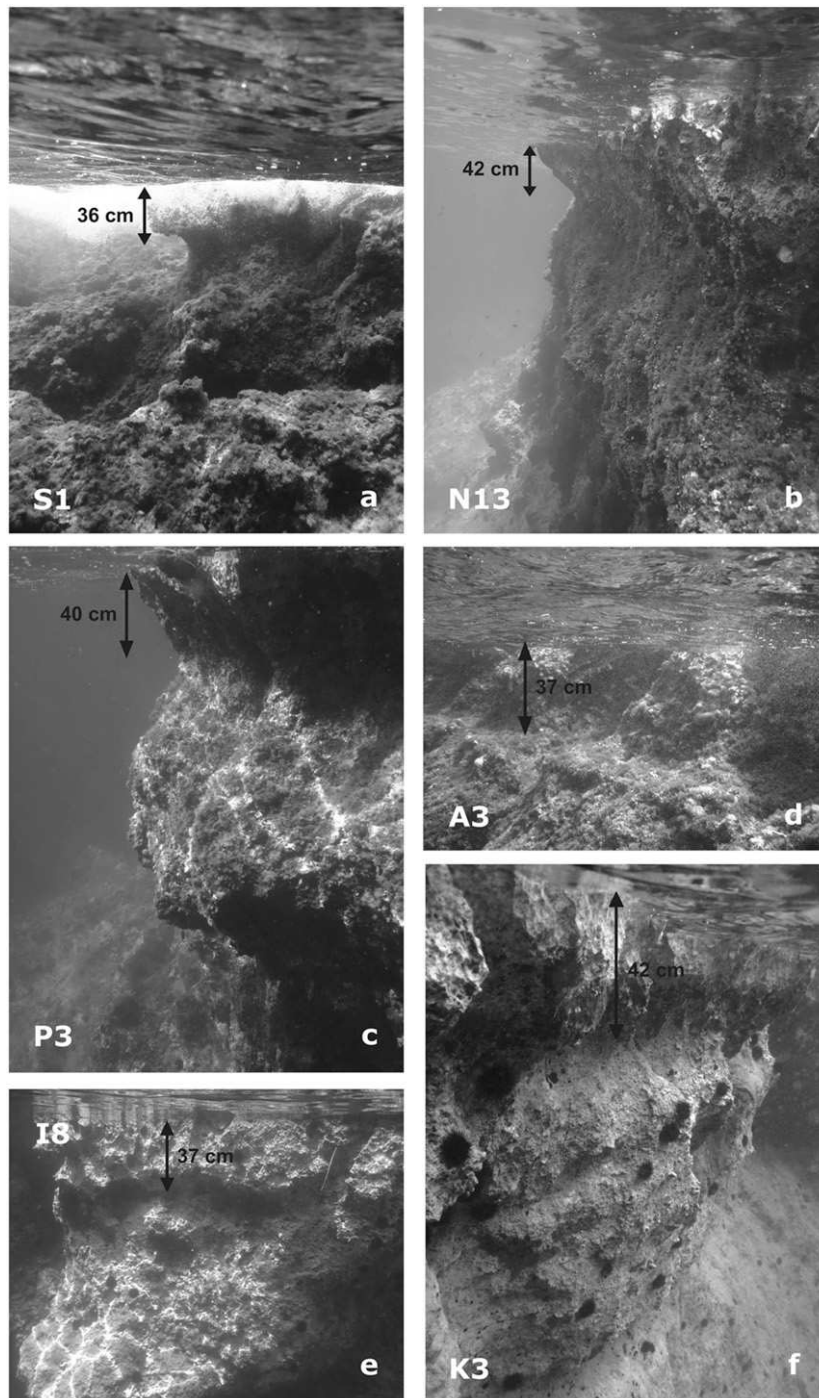
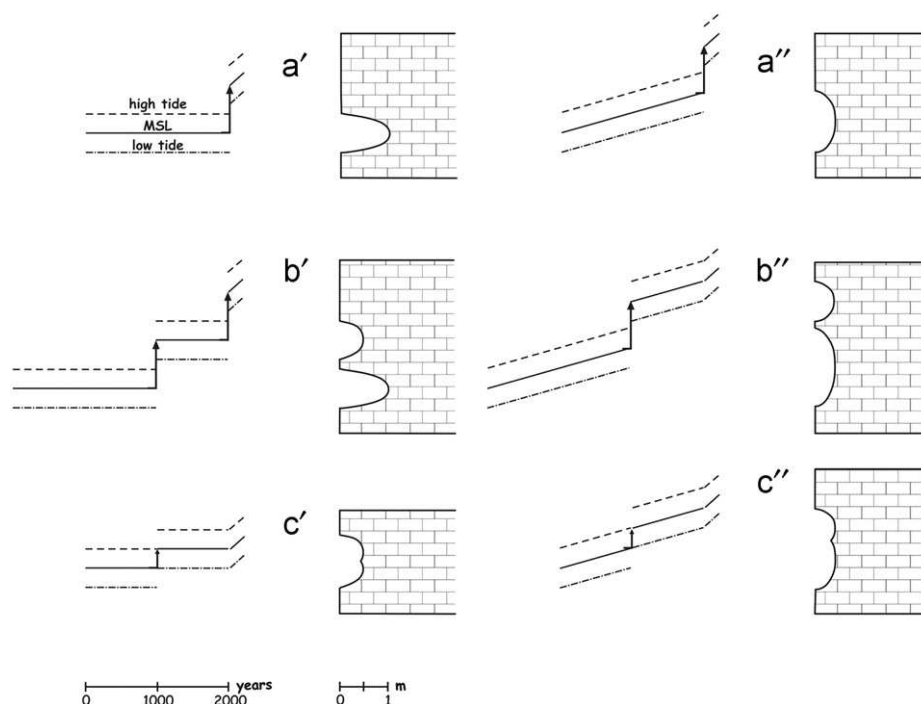


Fig. 3. The upper submerged notch in the different studied islands. For locations of photographs, see Table 1.

At Naxos Island, at Site N9 a regular tidal notch is developed with a vertex at  $-35 \pm 10$  cm. The 24 cm inward depth of the notch profile suggests the occurrence of a relatively stable sea-level during a period between 2.4 centuries and 12 centuries, depending on the rate of bioerosion, to enable its full development. At Site N10 the vertex of the upper notch is situated at  $-20 \pm 10$  cm. The 32 cm inward depth of the notch profile suggests the occurrence of a relatively stable sea-level during a period between 3.2 centuries and 16 centuries, depending on the rate of bioerosion, to enable its full development. At Site N12, the upper notch has been recognised with a vertex at about  $-30 \pm 10$  cm but the inward depth of vertex of 15 cm suggests the occurrence of a relatively stable sea-level during a period between 1.5 centuries and 7.5 centuries. The

b'-type (Evelpidou et al., 2011a) (Fig. 4) of the aforementioned notches suggests a rapid subsidence, greater than the tidal range, preceded by a relative sea-level stability. At Site N13 (Fig. 3(b)), the upper notch has been recognised with a vertex at about  $-42 \pm 10$  cm but an inward depth of vertex of 20 cm suggests the occurrence of a relatively stable sea-level during a period between 2 centuries and 1 millennium. The c'-type (Evelpidou et al., 2011a) (Fig. 4) suggests a rapid subsidence (smaller than the tidal range), preceded and followed by a relative sea-level stability, which produces a notch in the new intertidal range and afterwards shifts the former notches underwater.

At Iraklia Island, at Site I2, a very clear tidal upper notch can be observed. Its vertex is at  $27 \pm 10$  cm below sea-level and its inward



**Fig. 4.** Schema with theoretical notch geometries under different conditions. The left column illustrates the notch formations associated with rapid subsidence over time. Type a' corresponds to a reclinable U-shaped notch profile with the height of the notch roof ( $H_r$ ) very similar to the height of the notch floor ( $H_f$ ). This fossil notch has been preserved underwater after a rapid subsidence movement, greater than the tidal range, which followed a former relative sea-level stability. Type b' corresponds to two submerged fossil notches which preserved underwater after two rapid subsidence movements, greater than the tidal range. Type c' represents a fossil notch higher than the tidal range with two vertices, separated by an undulation in the notch profile. The notch sunk because of a rapid subsidence, smaller than the tidal range, preceded and followed by a relative sea-level stability. Thus, the two vertices indicate the former and the following MSL positions. The right column illustrates the same phenomena under gradual subsidence. Type a'' notch has been preserved underwater after a rapid subsidence movement. Before the rapid subsidence a gradual one took place, slower than the bioerosion rate, which resulted in a notch height greater than the tidal range. Type b'' fossil notches preserved underwater after two subsidence movements, greater than the tidal range. Before each of those two subsidence movements a gradual subsidence took place resulting in a notch height greater than the tidal range. Type c'' notch sunk because of a rapid subsidence, preceded by a gradual subsidence which expanded notch height. The rapid subsidence was smaller than the tidal range, preceded and followed by a relative sea-level stability.

depth is about 5 cm suggesting the occurrence of a relatively stable sea-level during a period between half a century and 2.5 centuries. At Site I3, an upper notch exists, with a vertex at  $45 \pm 10$  cm below sea-level. Its inward depth is 14 cm and suggests the occurrence of a relatively stable sea-level during a period between 1.4 centuries and 7 centuries. At Site I8, the inward depth of about 20 cm is developed between  $-20 \pm 10$  and  $-55 \pm 10$  cm (Fig. 3(e)), suggesting the occurrence of a relatively stable sea-level during a period between 2 centuries and 1 millennium. All notches of the aforementioned sites belong to b'-type (Evelpidou et al., 2011a) suggesting under the assumed conditions a rapid subsidence, greater than the tidal range, preceded by a relative sea-level stability (Fig. 4).

At Keros Island, at Site K3 (Fig. 3(f)), the upper submerged notch could be recognised, which is well and continuously developed from about  $-20 \pm 10$  to  $-50 \pm 10$  cm. The inward depth of about 15 cm suggests the occurrence of a relatively stable sea-level during a period between 1.5 centuries and 7.5 centuries. At Site K4, the roof of the upper notch is marked between  $-20 \pm 10$  and  $-49 \pm 10$  cm, while the vertex is at  $-34$  cm. The same inward depth with that of the preceding one site, suggests the same duration of relatively stable sea level. All notches of the aforementioned sites belong to b'-type (Evelpidou et al., 2011a) suggesting a rapid subsidence, greater than the tidal range, preceded by a relative sea-level stability (Fig. 4).

## 5. Discussion

It can be inferred that the presently submerged notch developed in the intertidal range, with an almost stable sea level, during

a period sufficiently long to acquire an inward depth of 18.5 cm on average, though there is a local variability between 5 and 35 cm that can be due, at least in part, to the rock type, the slope of the cliff and irregularities in the rock surface. The vertical position of the vertex may be used to attempt a qualitative estimation of the sea-level position before the submergence, while its inward depth may provide information on the duration of relative stable sea level necessary for the notch formation. The different type of notch profiles (a', with absence of lower notches) at Sifnos and Antiparos suggests the possibility of a different tectonic history.

In all the area considered, the vertex of the upper submerged notch – most often 30–40 ( $\pm 10$ ) cm below the present sea level – suggests that submergence could be the result of a double phenomenon: (i) the recent global sea-level rise, and (ii) a seismic subsidence displacement.

### 5.1. Evidence of a recent global sea-level rise

The submergence observed may reflect an effect of the global sea-level rise of 19 cm that occurred during the 20th century (Jevrejeva et al., 2008), often (especially since 1930: Church and White, 2006) at a rate faster than the possibilities of bioerosion. According to satellite altimetry the rate of the sea-level rise increased even to  $3.3 \pm 0.4$  mm/yr after 1993 (Cazenave and Llovel, 2010). Though it is known that the global sea-level rise did not occur uniformly around the world, it can be assumed that also in the Eastern Mediterranean it followed, more or less and eventually with a slight delay, the global trend.

If only the time period with tide-gauge records is considered, it appears that the global sea-level rise since 1870 (estimated to

1.7 ± 0.3 m by Church and White, 2006), has been a little slower along the Atlantic coasts of Europe, 1.44 ± 0.13 mm/yr since 1860 at Liverpool, (Woodworth, 1999); 1.32 ± 0.07 since 1861 at Brest (Pouvreau, 2008); and 1.37 ± 0.08 since 1860 at the Antioche straits (La Rochelle area) (Gouriou, 2012).

Among the longest tide-gauge records available in the Mediterranean at the PSMSL data bank, Marseille (France) shows between 1885 and 2009 (6 annual values missing) a rate of relative sea-level rise 1.239 mm/yr ( $R^2=0.6814$ ), while in Italy Trieste (between 1905 and 2011 with 6 annual values missing) shows a similar rate of about 1.229 mm/yr ( $R^2=0.522$ ). In the Aegean area, tide-gauge records seem available only since 1969. At Alexandroupolis, between 1969 and 2011 (11 annual data missing), the rate of relative MSL rise is 2.343 mm/yr ( $R^2=0.3548$ ), while at Syros in the Cyclades, between 1969 and 2010 (20 annual values missing), it is of 4.464 mm/yr ( $R^2=0.569$ ).

If a slight global sea-level rise seems to have started in the early 18th century (Jevrejeva et al., 2008) an acceleration in the rate of rise is generally situated during the second half of the 19th century, around 1865 (Kemp et al., 2011), or around 1890 (Wöppelmann et al., 2006; Pouvreau, 2008).

All the above rates of sea-level rise are clearly greater than the expected rates of bioerosion in carbonate rocks in the Mediterranean. It can be inferred that the presently submerged notch developed in the intertidal range, with an almost stable sea level, during a period sufficiently long to acquire an average inward depth of 18.5 cm, though there is a local variability between 5 and 35 cm that can be due, at least in part, to the rock type, the slope of the cliff and irregularities in the rock surface. An inward depth of 18.5 cm may correspond, under assumptions specified above of a bioerosion rate between 0.2 and 1 mm/yr (Evelpidou et al., 2011a), to a period of sea-level stability between 185 and 925 years long, that preceded the submergence of the notch. An approximate age for the period of development of the tidal notch can be deduced from the radiocarbon age of 232 ± 35 years BP (i.e., at AD 1718 ± 35) shown by *Cerastoderma* shell collected at a depth of 55 cm by core NA2 collected at Naxos near St. Georgios (Evelpidou et al., in press). At that time the submergence of the notch had probably not yet started.

If a slight gradual relative sea-level rise at a rate smaller than the bioerosion rate occurred during this period, its effect would have been not to submerge the notch, but to increase upwards the height of its profile and to slightly displace upwards the notch vertex, while decelerating the inward deepening rate of the notch profile would have been slowed down (Fig. 4).

The total sea-level rise at a rate greater than the possibilities of bioerosion can be therefore estimated to about 25 cm since 1865 (14 cm between 1865 and 1956 and 11 cm since 1956). An additional

subsidence of about 10 cm induced by the coseismic effect of an earthquake either before 1865, or in 1956, should be added.

## 5.2. Seismic deformation modelling

In an attempt to investigate the possible cause of this subsidence the historical earthquakes with  $M_s > 6$  having occurred in the area are summarised in Fig. 1(c) and Table 2. The number of earthquake candidates to have released the necessary energy appears quite limited. The most recent earthquake, near Milos Island in 2002, does not seem strong enough to have caused uniform subsidence as far as 130 km away. The 1934 earthquake occurred near Thera, is also unlikely to have caused subsidence in Cyclades, for the same reasons; in addition the 1934 earthquake was not considered important enough to be mentioned by Ambraseys and Jackson (1990) in their study of the seismicity of central Greece between 1890 and 1988. Information on the 1862 (Melos), 1733 (Sifnos) and 1735 (Melos) earthquakes, that could all have contributed to the submergence of the notch, is very limited. The Amorgos earthquakes of 1956 including the deeper aftershock with  $M_s=7.2$  following 13 min later the first shallow  $M_s=7.4$  shock, have been studied in more detail (Papadopoulos and Pavlidis, 1992; Stiros et al., 1994; Okal et al., 2009). For far-field sites remote from the Amorgos fault (Sifnos and Antiparos) the a'-type notch profile is consistent with only a single seismic event occurred either before the acceleration in the global sea level rise around 1865 (in 1733, or 1735, or 1862), or at the time of the Amorgos earthquake of 1956, excluding therefore the cumulative subsidence caused by two historical tremors. If an earthquake before 1865 has to be preferred, this would imply that Sifnos and Antiparos had a recent relative sea-level history different from that observed in the other islands considered.

A characteristic site indicating the uplift of Amorgos island is Aghia Anna beach where a bench of about 40 cm in height has been identified (Stiros et al., 1994). This island can be regarded in fact as the footwall block of a major normal fault (Papadopoulos and Pavlidis, 1992; Stiros et al., 1994; Okal et al., 2009). The rupture zone of this earthquake, which trends NE–SW and coincides with the Amorgos Astypalea trough, seems to belong to a set of similar faults that characterize the eastern Aegean, while part of the central and south Aegean have been regarded rather as an “aseismic plateau” (e.g., Morelli et al., 1975). One may speculate about the manner of propagation of the recent subsidence through the Cycladic plateau in an apparently uniform manner along a distance of over 100 km.

A first possibility would be that the co-seismic subsidence observed has been the result of a fault reactivation breaking the Cycladic plateau.

**Table 2**  
Historical earthquakes with decreasing magnitude ( $> 6$ ) in the Cycladic islands area (Papazachos and Papazachou, 2003).

| Year AD | Time<br>Mmdd-hh-min | Long.  | Lat.   | Depth (km) | Magnitude | Code | Region  |
|---------|---------------------|--------|--------|------------|-----------|------|---------|
| 1956    | 0709-03-11          | 25.91  | 36.64  | 15         | 7.4       |      | Amorgos |
| 1956    | 0709-03-24          | 25.91  | 36.45  | 95         | 7.2       |      | Amorgos |
| 1650    | 1009-               | 25.5   | 36.5   |            | 7.0       | VIII | Thera   |
| 1862    | 0621-05-30          | 24.4   | 36.9   |            | 7.0       | VIII | Melos   |
| 46      |                     | 25.4   | 36.4   |            | 6.5       |      | Thera   |
| 1733    | 1223-15-            | 24.8   | 37.1   |            | 6.5       | VIII | Sifnos  |
| 1735    |                     | 24.5   | 36.8   |            | 6.5       | VIII | Melos   |
| 1891    | 05-11-              | 24.5   | 37.5   |            | 6.4       | VII  | Kithnos |
| 1934    | 1109-13-41          | 25.41  | 36.47  | 132        | 6.3       |      |         |
| 2002    | 05-21-20-53         | 24.273 | 36.635 | 106        | 6.3       | VII  |         |
| 1866    | 0131-               | 25.4   | 36.4   |            | 6.1       |      | Thera   |

However, a distance of over 100 km is much longer than the 20–30 km-long normal faults recognised in the Aegean region (Pavlidis and Caputo, 2004). This would imply the activation of more than one fault segments by earthquakes with  $M_s > 6$ , with vertical displacements of the various segments that may not have occurred all at the same time. According to this first possibility, part of the subsidence observed might have occurred earlier than 1956 (in 1862 or even in 1733).

A second possibility is that the Cycladic plateau reacted to the Amorgos earthquake as an almost rigid block causing several Cycladic islands to subside in a similar manner. As observed by Papadopoulos and Pavlidis (1992), during the 1956 Amorgos earthquake sequence a large portion of the lithospheric layer ruptured. The fault plane, striking along the major axis of the trough separating the islands of Amorgos and Astypalea, can be considered as a tectonic boundary for the Cycladic plateau and belongs to a set of parallel and similar faults that characterize the eastern Aegean. Amorgos Island can be considered as the uplifted and backtilted footwall of this tectonic boundary. As noted by Stiros et al. (1994), the movements of uplift and tilting of Amorgos Island seem superimposed on a regional lowering of the relief of the Cyclades. According to this second possibility the only rupture zone was that of the fault activated in 1956 offshore the eastern coast of Amorgos and it would have been sufficient to cause an almost uniform co-seismic subsidence in most eastern islands of the Cycladic plateau that reacted elastically as an almost rigid body. However, this second possibility seems unrealistic because, with such a model,

the subsidence should have rapidly decreased moving away from the fault area (S.C. Stiros, personal communication).

A third possibility of explanation is that a co-seismic deformation was followed by fast post-seismic movements due to the viscous relaxation of ductile asthenospheric layers, which enhanced the co-seismic effect. Post-seismic deformations in Greece seem not to be large, as discussed by Feng et al. (2010) for the Achaia–Elia 2008 earthquake (Northwestern Peloponnese), or by Stiros and Rondogianni (1985) for the Atalandi Fault Zone. In Cycladic area, however, Westaway (2002) suggested the presence of a low-viscosity layer; according to his computations, a viscosity not exceeding  $10^{18}$  Pa s at the base of the crust is needed in order to explain the constant depth of the Moho in the tectonic framework of the region (Tirel et al., 2004; Sodoudi et al., 2006). Ambraseys and Jackson (1990) mention that the Amorgos 1956 seismic event was followed by aftershocks that continued for almost seven months. Aftershocks are usually supposed to be very close or even on the rupture area and are therefore unlikely to have caused subsidence over a wide area. However, the first aftershock, occurred 13 min after the main event, ruptured at a depth of about 100 km and had an energy release comparable with that of the mainshock (Papadopoulos and Pavlidis, 1992); it may have therefore efficiently excited relaxation modes in deep ductile layers, resulting in a wide postseismic subsidence affecting the whole area.

In order to explore these possibilities, we carried out a numerical simulation of the co-seismic and post-seismic deformations following the Amorgos earthquake, using a semi-analytical

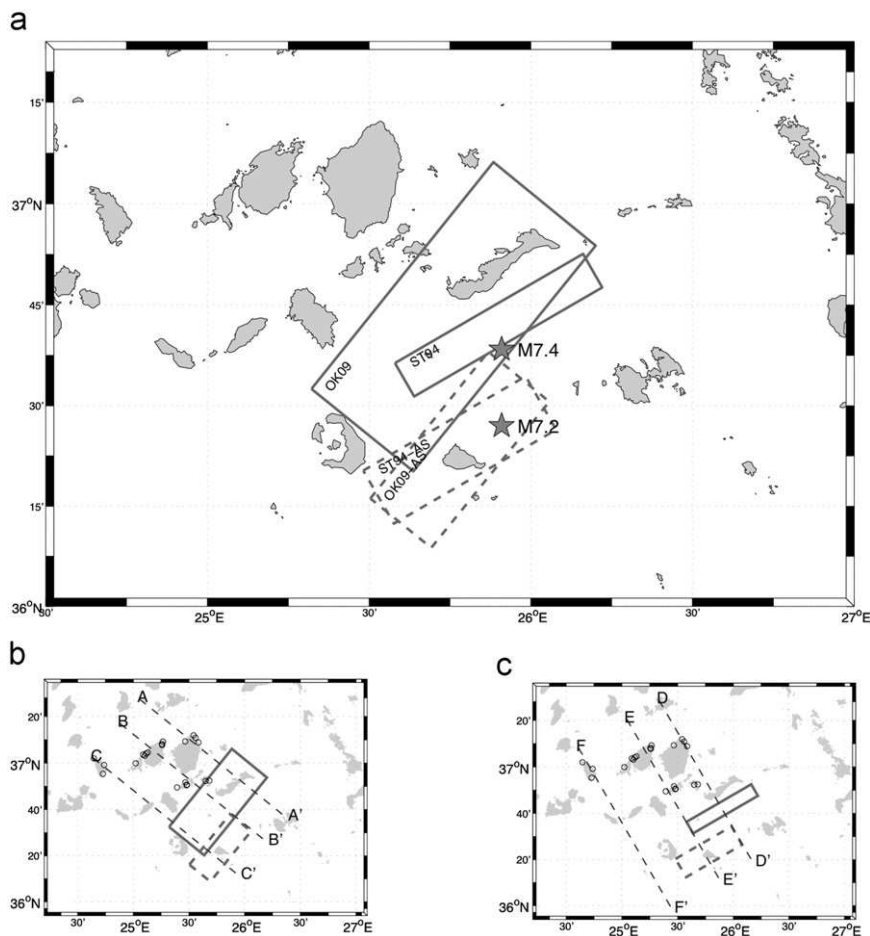


**Fig. 5.** (a) Position and extents of the considered fault models. Mainshock faults according to Stiros et al. (1994) and Okal et al. (2009) are labelled ST94 and OK09 and drawn with solid lines. Aftershock faults are labelled with ST94-AS and OK09-AS and drawn with dashed lines. Two stars mark the location of the  $M=7.4$  mainshock and of the  $M=7.2$  aftershock according to Papazachos and Papazachou (2003). (b) and (c) Cross-sections used to plot the profiles of Figs. 10 and 11, for fault models OK09 (frame b) and ST94 (frame c). The position of notch sites are marked with circles.

model of the post-seismic response of a spherical, layered, self-gravitating Earth to a seismic dislocation (Piersanti et al., 1995; Melini et al., 2008).

We assumed an elastic stratification with the structure of PREM (Dziewonski and Anderson, 1981), with a Moho depth of 25 km and a lithospheric–asthenospheric boundary at 100 km

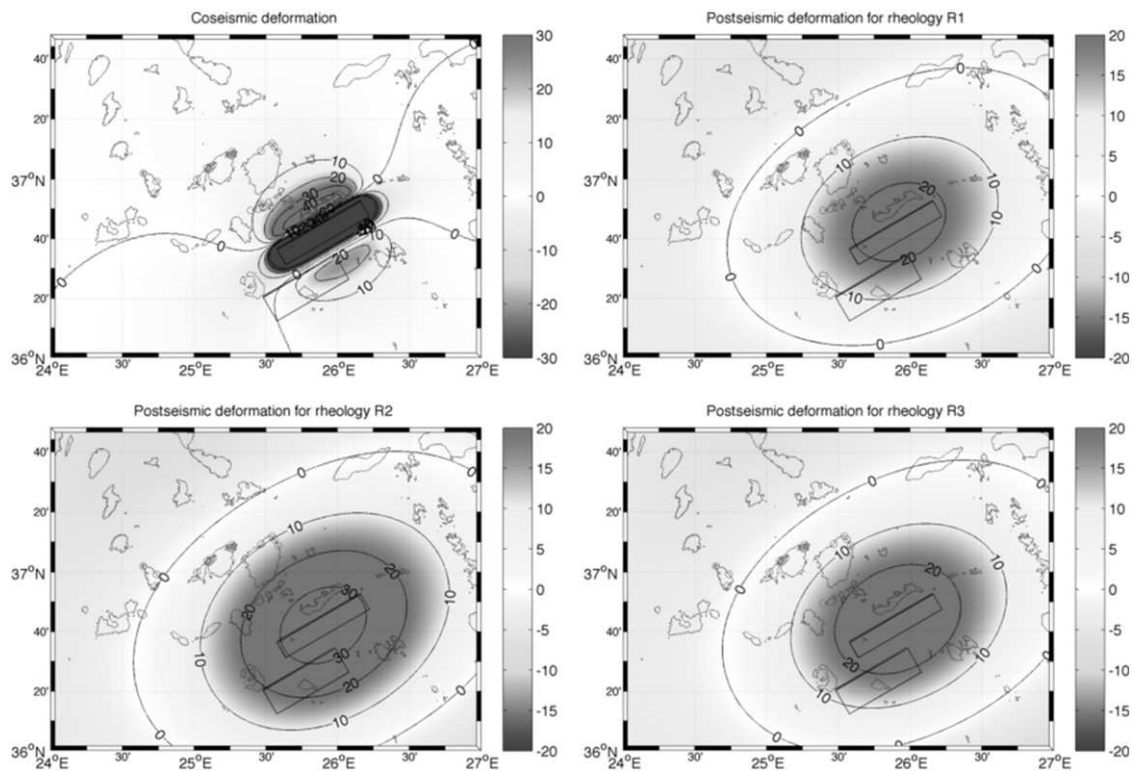


**Fig. 6.** Modelled co-seismic (top left) and post-seismic deformation following the 1956 Amorgos earthquake for the three considered rheology models, using the fault model by Stiros et al. (1994) and including the  $M$  7.2 aftershock. Post-seismic deformation is evaluated at August 1, 2010. Scale units are in cm. A rectangle marks the surface projection of the seismic source; small circles show the location of measurement sites.

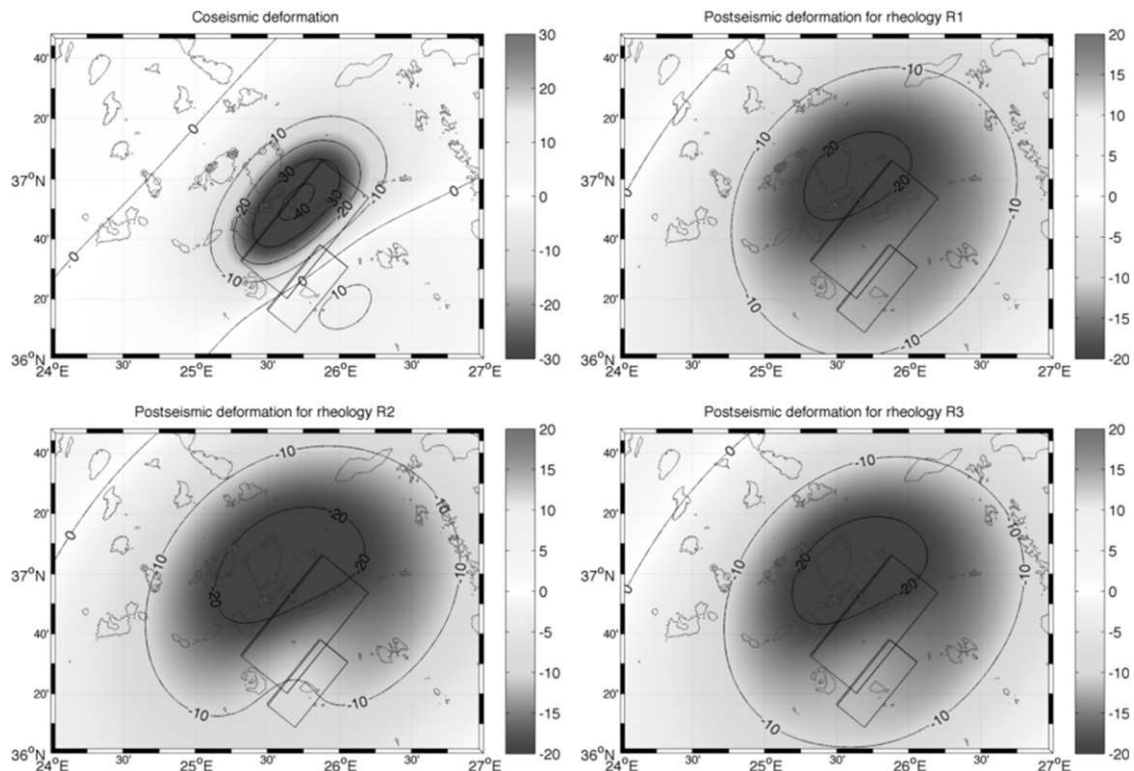


**Fig. 7.** Modelled co-seismic (top left) and post-seismic deformation following the 1956 Amorgos earthquake for the three considered rheology models, using the fault model by Okal et al. (2009) and including the  $M$  7.2 aftershock. See also caption of Fig. 6.

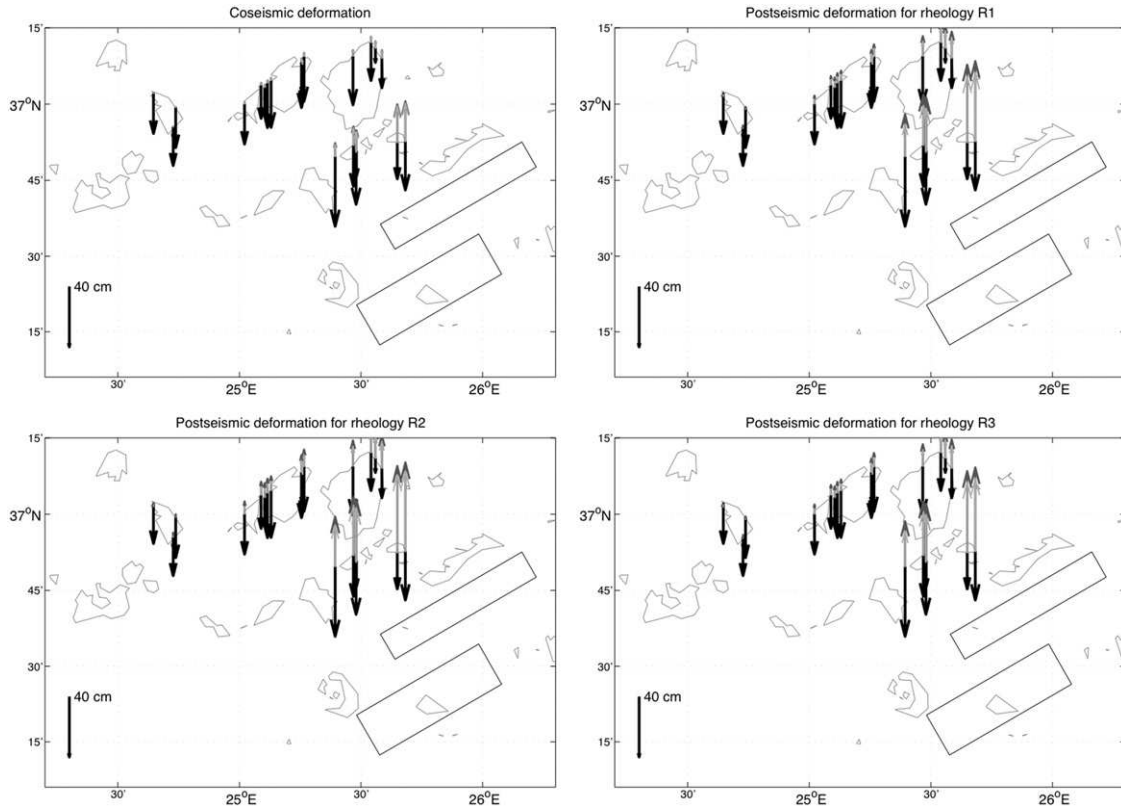


**Fig. 8.** Modelled and observed subsidence at the measurement sites for the ST94 fault models. Black vectors represent observed subsidence after sea-level rise correction. Dark and light grey vectors represent predicted subsidence for the mainshock alone and the combination of mainshock and aftershock, respectively. Rectangles mark the surface projection of the seismic sources.

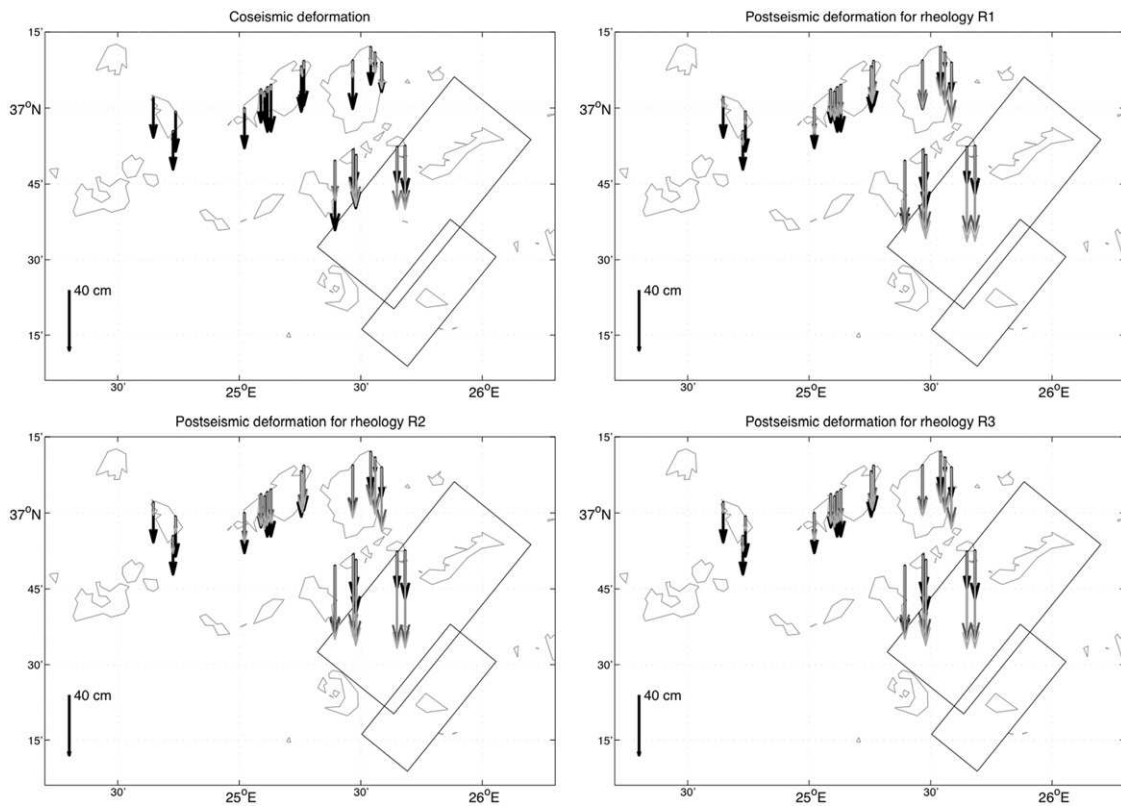


**Fig. 9.** Modelled and observed subsidence at the measurement sites for the OK09 fault models. See also caption of Fig. 8.

depth (Sodoudi et al., 2006). We defined a low-viscosity layer between 60 and 100 km depths, immediately below the seismogenic layer (Chouliaras, 2009), and experimented three rheology models: a Burgers rheology with transient viscosity  $5 \times 10^{17}$  Pa s and steady-state viscosity  $10^{19}$  Pa s (R1 hereinafter) and two Maxwell rheologies with viscosities  $10^{17}$  and  $10^{18}$  Pa s (R2 and R3 hereinafter). For all three models, the asthenosphere and upper mantle have Maxwell rheologies with viscosities  $10^{19}$  and  $10^{20}$  Pa s, respectively.

For the 1956 Amorgos earthquake, two rupture models have been proposed. The first, by Stiros et al. (1994) (ST94 hereinafter), assumes a shallow rupture plane on the basis of fossil deposits and aerial photographic surveys; the latter, by Okal et al. (2009) (OK09 hereinafter), uses mantle wave data and tsunami observations to infer a deeper (45 km) rupture process. We computed vertical deformation predictions with the two rupture models, both considering the mainshock alone and including the aftershock contribution. The rupture plane for the aftershock has been defined by assuming the same geometrical orientation of the mainshock, and using the empirical relations by Wells and Coppersmith (1994) for the other parameters. The considered faulting scenarios are depicted in Fig. 5(a).

The surface displacement field corresponding to the two faulting models are shown in Figs. 6 and 7. The field shows the

superposition of mainshock and aftershock effects. The ST94 fault model (Fig. 6) results in a coseismic tilting, with the axis separating uplift from subsidence roughly located along the SE coast of the Amorgos island; all the surveyed sites are located in an uplifted area. The postseismic effect results in a further uplift for all the islands, except at Sifnos which shows a slight postseismic subsidence. On the other hand, with the OK09 fault model (Fig. 7), we obtain a wide coseismic subsidence area with peak values between the Amorgos and Keros islands, followed by a further postseismic covering the whole region, with largest deformation values for rheologies R2 and R3.

In Figs. 8 and 9 we compare the observed subsidence (black vectors) with modelled co-seismic and post-seismic deformations obtained for fault models ST94 and OK09, respectively. We show separately model predictions obtained using only the mainshock (dark grey vectors) and using a superposition of mainshock and aftershock (light grey vectors). The observed subsidence plotted in Figs. 8 and 9 has been corrected to account for the global sea-level rise that occurred in the 19th century (Church and White, 2006; Jevrejeva et al., 2008; Cazenave and Llovel, 2010) by subtracting a constant offset of 11 cm from observed data. In Figs. 10 and 11 we show the modelled vertical deformation for fault models ST94 and OK09, respectively, on the cross-sections shown in Fig. 5(b) and (c), for both coseismic and postseismic

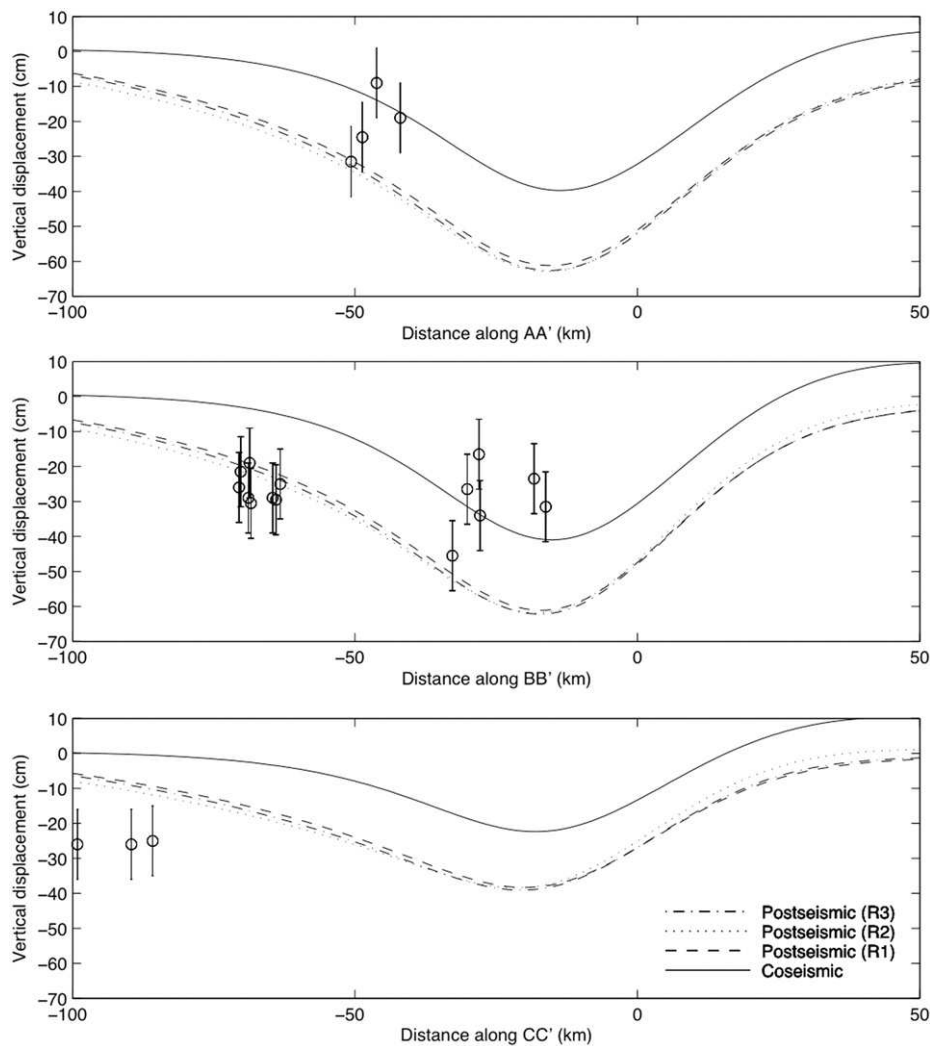


**Fig. 10.** Modelled vertical deformation along cross-sections DD', EE' and FF' (see Fig. 5) for the ST94 faulting model, using all the considered rheology models. Distances are measured from the fault strike axis; negative and positive distances are towards NW and SE directions, respectively. Observed vertical deformation at notch sites is projected on the nearest cross-section.

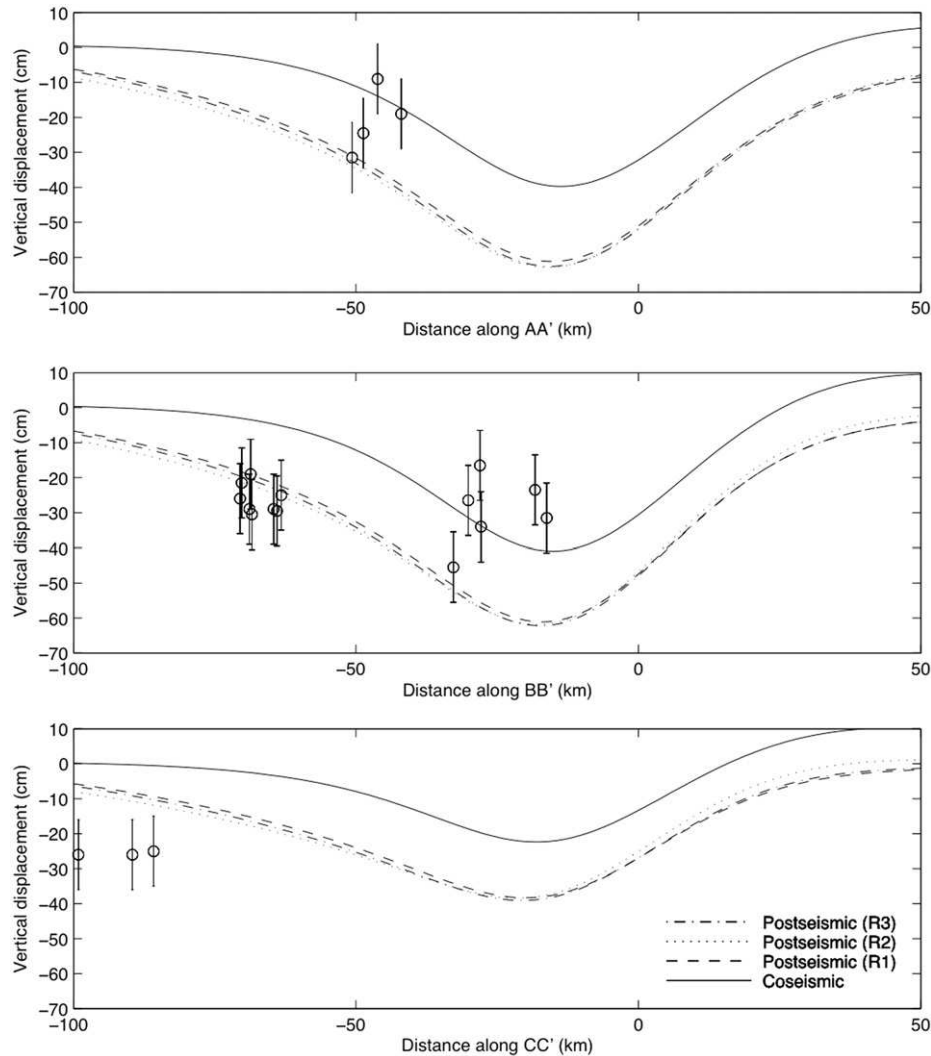


Fig. 11. Modelled vertical deformation along cross-sections AA', BB' and CC' (see Fig. 5) for the OK09 faulting model. See also caption of Fig. 10.

responses, taking into account both mainshock and aftershock effects. The measured deformation at notch sites is projected on the nearest cross-section and shown in Figs. 10 and 11 for comparison.

As discussed above, the coseismic response predicts on the considered sites an uplift for the ST94 model and a subsidence for the OK09 model. In both cases the signal strongly decays with distance from epicentre, so that with model OK09 we reproduce observed offsets only on the nearest islands (Keros and Iraklia). The inclusion of post-seismic relaxation generally enhances the co-seismic signal leading to a further subsidence or uplift for the OK09 and ST94 models, respectively. The inclusion of the  $M=7.2$  aftershock in the models results in a (small) subsidence on all the notch sites, leading to an amplification of the subsidence for the OK09 model and in a smaller uplift for the ST94 model.

From these results, the faulting model by Stiros et al. (1994) seems to be not consistent with all our observations, even if we stress that it is fully consistent with local tectonics and supported by field evidences.

Focusing on the OK09 model, we see that the inclusion of postseismic effects results in a subsidence signal that is less strongly decaying with distance. In particular, the modelled subsidence is in good agreement with observations at Naxos, Iraklia and Paros sites, while it is overestimated at Keros and underestimated at the most distant sites (Sifnos). Okal et al. (2009)

suggested the possibility of an aseismic uplift of the Amorgos island in order to reconcile the regional subsidence predicted by their model with the uplift evidences found by Stiros et al. (1994). This hypothesis could also explain the overestimation of modelled deformations at Keros, which would be counterbalanced by the aseismic movements.

From Figs. 10 and 11 we may see that the observed subsidence shows no clear trend with distance from the fault strike axis, even if the geographical distribution of sites does not give a complete coverage of modelled distances. While the ST94 model (Fig. 10) predicts an uplift at all the surveyed sites, as discussed above, with the OK09 model (Fig. 11) subsidence at sites located between 50 and 80 km from the fault strike axis is well reproduced by postseismic models. This result suggests that at Paros and Antiparos postseismic relaxation following the Amorgos earthquake might be responsible for the observed subsidence, while at the other sites local phenomena may be superimposed to the modelled values.

From a visual inspection of Fig. 9 we cannot identify a preferred rheology model. However, the lowest root mean square of residuals is obtained for rheology R1, which is characterised by a Burgers rheology with a low transient viscosity ( $5 \times 10^{17}$  Pa s). This is in agreement with the results by Westaway (2002), who invoked a low-viscosity lithospheric layer in order to explain the absence of Moho topographic features.

With all the considered rheologies, we are not able to fit the far-field measurements at the Sifnos island. These sites could be affected by a large-scale postseismic deformation induced by the Ms 7.2 aftershock, if a more efficient excitation of relaxation modes is present. However, due to weak constraints both on the geometry of the aftershock rupture plane and on the detailed rheological structure it is not possible to give a definite answer on this point.

## 6. Conclusions

The submarine geomorphological survey along the coasts of Sifnos, Antiparos, Paros, Naxos, Iraklia and Keros revealed the absence of a tidal notch at the present sea level while, with an accuracy of  $\pm 10$  cm, a well developed submerged notch is existing on average at  $-35 \pm 10$  cm below the present sea level. This submerged notch has a mean inward depth of 18.5 cm, which may correspond, assuming it formed in a uniform lithological, biological and climatic conditions among the various islands, during a period of relative sea-level stability between 185 and 925 years long, that has been subsequently interrupted by a submergence of 30–40 cm affecting this wide area. We ascribed about two thirds the observed submergence to the recent global sea-level rise occurred during the last two centuries, while about one decimetre should be ascribed to recent seismic effects.

We investigated the effect of the Amorgos earthquake as a possible explanation for part of the observed subsidence. The faulting model by Stiros et al. (1994) predicts an uplift at all the surveyed sites and is therefore not consistent with our data. The model proposed by Okal et al. (2009), with all the explored rheology models, largely overestimates observations at the nearest sites (Keros island) and slightly overestimate far-field deformations, while is consistent with observed subsidence at Paros and Antiparos. A possible explanation is that near-field sites could be affected by an aseismic uplift along secondary shallow faults, as suggested also by Okal et al. (2009), while far-field sites could be affected by vertical deformation caused by other older earthquakes or by local tectonic effects.

## Acknowledgements

We wish to thank the Municipalities of Paros, Naxos, Iraklia and Koufonissia for the facilities granted to our underwater survey, and Prof. Stathis Stiros (University of Patras) for useful suggestions. We also thank the Hellenic Hydrographic Service for providing hourly tidal records at Sifnos. Field work has been supported in part by COST Action ES 0701 "Improved constraints on models of Glacial Isostatic Adjustment". Constructive suggestions of two anonymous reviewers have much contributed to improve a previous version of this work.

## References

- Ambraseys, N.N., Jackson, J.A., 1990. Seismicity and associated strain of central Greece between 1890 and 1988. *Geophysical Journal International* 101, 663–708.
- Caputo, R., Pavlides, S., Papadopoulos, G., Helly, B., 1998. Palaeoseismological researches in northern Thessaly, Greece. Preliminary Results: XXVI. General assembly of the ESC, Tel Aviv, August 23–28, 1998. Abstracts, p. 25.
- Cazenave, A., Llovel, W., 2010. Contemporary sea level rise. *Annual Review of Marine Science* 2, 145–173.
- Chatzipetros, A., Pavlides, S., Mountrakis, D., 1998. Understanding the 13 May 1995 western Macedonia earthquake: a paleoseismological approach. *Journal of Geodynamics* 26, 327–339.
- Chouliaras, G., 2009. Investigating the earthquake catalog of the National Observatory of Athens. *Natural Hazards Earth System Sciences* 9, 905–912.
- Church, J.A., White, N.J., 2006. A 20th century acceleration in the global sea-level rise. *Geophysical Research Letters* 33, L01602. <http://dx.doi.org/10.1029/2005GL024826>.
- Desruelles, S., Fouache, E., Ciner, A., Dalongeville, R., Pavlopoulos, K., Kosun, E., Coquinot, Y., Potdevin, J.-L., 2009. Beachrocks and sea level changes since Middle Holocene: comparison between the insular group of Mykonos–Delos–Rhenia (Cyclades, Greece) and the southern coast of Turkey. *Global and Planetary Change* 66 (1–2), 19–33.
- Doutsos, Th., Kokkalas, S., 2001. Stress and deformation patterns in the Aegean region. *Journal of Structural Geology* 23, 455–472.
- Dziewonski, A.M., Anderson, D.L., 1981. Preliminary reference Earth model. *Physics of the Earth and Planetary Interiors* 25, 297–356.
- Evelpidou N., Pavlopoulos K., Vassilopoulos A., Triantafyllou M., Vouvalidis K., Syrides G., Holocene palaeogeographical reconstruction of the western part of Naxos island (Greece), *Quaternary International*, in press.
- Evelpidou, N., Pirazzoli, P.A., Vassilopoulos, A., Tomasin, A., 2011a. Holocene submerged shorelines on Theologos area (Greece). *Zeitschrift für Geomorphologie* 55, 31–44.
- Evelpidou, N., 2001. Geomorphological and environmental study of Naxos Island using remote sensing and GIS. PhD Thesis, University of Athens, Faculty of Geology, Department of Geography and Climatology, GAIA, Vol. 13, p. 226.
- Evelpidou, N., Pirazzoli, P.A., Saliège, J.F., Vassilopoulos, A., 2011b. Submerged notches as evidence for Holocene subsidence of the northern Corinth Gulf (Greece). *Continental Shelf Research* 31, 1273–1281.
- Feng, L., Newman, A.V., Farmer, G.T., Psimoulis, P., Stiros, S.C., 2010. Energetic rupture, coseismic and postseismic response of the 2008 MW 6.4 Achaia–Elia Earthquake in Northwestern Peloponnese, Greece: an indicator of an immature transform fault zone. *Geophysical Journal International* 183, 103–110.
- Flemming, N.C., Webb, C.O., 1986. Tectonic and eustatic coastal changes during the last 10,000 years derived from archaeological data. *Zeitschrift für Geomorphologie* N.F. 62, 1–29.
- Gaki-Papanastassiou, K., Evelpidou, N., Maroukian, H., Vassilopoulos, A., 2010. Palaeogeographic evolution of the Cyclades islands (Greece) during the Holocene. In: Green, David R. (Ed.), *Coastal and Marine Geospatial Technologies*. Springer copyright, pp. 297–304.
- Galanopoulos, G.A., 1981. The damaging shocks and the earthquake potential of Greece. *Annals Geology Pays Hell* 30, 647–724.
- Goldsworthy, M., Jackson, J., Haines, J., 2002. The continuity of active fault systems in Greece. *Geophysical Journal International* 148, 596–618.
- Gouriou, T., 2012. Evolution des composantes du niveau marin à partir d'observations de marégraphie effectuées depuis le fin du 18e siècle en Charente Maritime. Thèse de doctorat, Université de La Rochelle, 482 p.+ Annexes.
- Guidoboni, E., Comastri, A., Traina, G., 1994. Catalogue of Ancient Earthquakes in the Mediterranean Area Up to 10th Century. ING-SGA, Bologna, p. 504.
- Jevrejeva, S., Moore, J.C., Grinstead, A., Woodworth, P.J., 2008. Recent global sea level acceleration started over 200 years ago? *Geophysical Research Letters* 35, L08715. <http://dx.doi.org/10.1029/2008GL033611>.
- Kemp, A.C., Horton, B.P., Donnelly, J.P., Mann, M.E., Vermeer, M., Rahmstorf, S., 2011. Climate related sea-level variations over the past two millennia. *Proceedings of the National Academy of Sciences* 108, 11017–11022.
- Laborel, J., Laborel-Deguen, F., 2005. Sea-level indicators, biological. In: Schwartz, M.L. (Ed.), *Encyclopedia of Coastal Science*. Springer, pp. 833–834.
- Lykousis, V., 2009. Sea-level changes and shelf break prograding sequences during the last 400ka in the Aegean margins: subsidence rates and paleogeographic implications. *Continental Shelf Research* 29, 2037–2044.
- Lykousis, V., Anagnostou, C., Pavlakis, P., Rousakis, G., Alexandri, M., 1995. Quaternary sedimentary history and neotectonic evolution of the eastern part of Central Aegean Sea, Greece. *Marine Geology* 128, 59–71.
- McKenzie, D., 1978. Active tectonics of the Alpine-Himalayan belt: the Aegean Sea and surrounding regions. *Geophysical Journal of the Royal Astronomical Society* 55, 217–254.
- Melini, D., Cannelli, V., Piersanti, A., Spada, G., 2008. Post-seismic rebound of a spherical Earth: new insights from the application of the Post-Widder inversion formula. *Geophysical Journal International* 174, 672–695.
- Mercier, J.-L., Sorel, D., Vergely, P., Simeakis, K., 1989. Extensional tectonic regimes in the Aegean basins during the Cenozoic. *Basin Research* 2, 49–71.
- Morelli, C., Pisani, M., Gantar, C., 1975a. Geophysical studies in the Aegean Sea and in the Eastern Mediterranean. *Bollettino Geofisica Teor. Applied* 18, 127–167.
- Morelli, C., Pisani, M., Gantar, C., 1975b. Geophysical studies in the Aegean Sea and in the Eastern Mediterranean. *Bollettino Geofisica Teor. Applied* 18, 127–167.
- Morhange, C., Pirazzoli, P.A., Marriner, N., Nammour, T., Montaggioni L.F., 2006. Late Holocene relative sea-level changes in Lebanon, Eastern Mediterranean. *Marine Geology* 230, 99–114.
- Okal, E., Synolakis, C., Uslu, B., Kalligeris, N., Voukoulalas, E., 2009. The 1956 earthquake and tsunami in Amorgos, Greece. *Geophysical Journal International* 178, 1533–1554.
- Pantosti, D., Collier, R., D'Addezio, G., Masana, E., Sakellariou, D., 1996. Direct geological evidence for prior earthquakes on the 1981 Corinth fault (Central Greece). *Geophysical Research Letters* 23, 3795–3798.
- Papadopoulos, G., Pavlidis, S., 1992. The large 1956 earthquake in the South Aegean: macroseismic fields configuration, faulting and neotectonics of Amorgos Island. *Earth and Planetary Science Letters* 113, 383–396.
- Papanikolaou, D., 1987. Tectonic evolution of the Cycladic blueschist belt (Aegean Sea, Greece). In: Helgeson, H.C. (Ed.), *Chemical Transport in Metasomatic Processes*. Kluwer, Dordrecht, pp. 429–450.

- Papanikolaou, D.J., Sabot, V., Papadopoulos, T., 1981. Morphotectonics and seismicity in the Cyclades, Aegean Sea. *Zeitschrift für Geomorphologie N.F.* 40, 165–174.
- Papazachos, B.C., 1990. Seismicity of the Aegean and surrounding area. *Tectonophysics* 178, 287–308.
- Papazachos, B.C., Papadopoulos, G.A., 1977. Deep tectonic and associated ore deposits in the Aegean area. *Proceedings 6th Colloquia Geology Aegean Region* 3, 1071–1080.
- Papazachos, B.C., Papazachou, C., 1997. *The Earthquakes of Greece*. Editions ZITI, Thessaloniki, p. 304.
- Papazachos, V., Papazachou, K., 2003. *Greek Earthquakes*, 3rd edn. Ziti, Thessaloniki, p. 288.
- Pavrides, S., 1996a. Active faults in Greece. *Journal of Earthquake Prediction Research* 5, 422–430.
- Pavrides, S., 1996b. First palaeoseismological results from Greece. *Annali di Geofisica* 34, 545–555.
- Pavrides, S., Caputo, R., 2004. Magnitude versus faults' surface parameters: quantitative relationships from the Aegean. *Tectonophysics* 380 (3–4), 159–188.
- Pavrides, S., Caputo, R., Chatzipetros, A., 2000. Empirical relationships among earthquake magnitude, surface ruptures and maximum displacement in the broader Aegean region. In: Panayides, I., Xenophontos, C., Malpas, J. (Eds.), *3rd International Conference on the Geology of the Eastern Mediterranean*. *Proceedings*, 159–168.
- Peterek, A., Schwarze, J., 2004. Architecture and Late Pliocene to recent evolution of outer-arc basins of the Hellenic subduction zone (south-central Crete, Greece). *Journal of Geodynamics* 38, 19–55.
- Piersanti, A., Spada, G., Sabadini, R., Bonafede, M., 1995. Global post-seismic deformation. *Geophysical Journal International* 120, 544–566.
- Pirazzoli, P.A., 1980. Formes de corrosion marine et vestiges archéologiques submergés: interprétations néotectonique de quelques exemples en Grèce et en Yougoslavie. *Annales Institut Océanographique* 56 (S), 101–111.
- Pirazzoli, P.A., 1986. Marine notches. In: van de Plassche, O. (Ed.), *Sea-Level Research: a Manual for the Collection and Evaluation of Data*. Geo Books, Norwich, pp. 361–400.
- Pirazzoli, P.A., 2005. Marine erosion features and bioconstructions as indicators of tectonic movements, with special attention to the eastern Mediterranean area. *Zeitschrift für Geomorphologie Suppl.* 137, 71–77.
- Pirazzoli, P.A., Laborel, J., Saliège, J.F., Erol, O., Kayan, I., Person, A., 1991. Holocene raised shorelines on the Hatay coasts (Turkey): palaeoecological and tectonic implications. *Marine Geology* 96, 295–311.
- Pouvreau, N., 2008. *Trois cents ans de mesures marégraphiques en France: outils, méthodes et tendances des composantes du niveau de la mer au port de Brest*. Thèse de doctorat. Université de La Rochelle, 474 p.
- Soudouki, F., Kind, R., Hatzfeld, D., Priestley, K., Hanka, W., Wylegalla, K., Stavrakakis, G., Vafidis, A., Harjes, H., Bohnhoff, M., 2006. Lithospheric structure of the Aegean obtained from P and S receiver functions. *Journal of Geophysical Research* 111, B12307. <http://dx.doi.org/10.1029/2005JB003932>.
- Stiros, S., 2005. Social and historical impacts of earthquake-related sea-level changes on ancient (prehistoric to Roman) coastal sites. *Zeitschrift für Geomorphologie* 137 (79–89), 2005.
- Stiros, S., Pirazzoli, P., 2004. Impact of short-wavelength sea-level oscillations on coastal biological zoning: evidence from Nisyros island (Aegean Sea), and implications for the use of the biological mean sea level as a Geodetic Datum. *Journal of Coastal Research* 20, 244–255.
- Stiros, S., Rondogianni, T., 1985. Recent vertical movements across the Atalandi fault-zone (Central Greece). *Pure and Applied Geophysics* 123, 837–848.
- Stiros, S.C., Laborel, J., Laborel-Deguen, F., Papageorgiou, S., Evin, J., Pirazzoli, P.A., 2000. Seismic coastal uplift in a region of subsidence: Holocene raised shorelines on Samos Island, Aegean Sea, Greece. *Marine Geology* 170, 41–58.
- Stiros, S.C., Marangou, L., Arnold, M., 1994. Quaternary uplift and tilting of Amorgos Island (southern Aegean) and the 1956 earthquake. *Earth and Planetary Science Letters* 128, 65–76.
- Stiros, S.C., Pirazzoli, P.A., Fontugne, M., 2009. New evidence of Holocene coastal uplift in the Strophades Islets (W Hellenic Arc, Greece). *Marine Geology* 267 (3–4), 207–211.
- Tirel, C., Gueydan, F., Tiberi, C., Brun, J.P., 2004. Aegean crustal thickness inferred from gravity inversion. *Geodynamical implications*. *Earth and Planetary Science Letters* 228, 267–280.
- Wells, D.L., Coppersmith, K., 1994. New empirical relationships among magnitude, rupture length, rupture width, rupture area, and surface displacement. *Bulletin of the Seismological Society of America* 84, 974–1002.
- Westaway, R., 2002. The Quaternary evolution of the Gulf of Corinth, central Greece: coupling between surface processes and flow in the lower continental crust. *Tectonophysics* 348, 269–318.
- Woodworth, P.L., 1999. A study of changes in high water levels and tides at Liverpool during the last 230 years with some historical background. Report No. 56, Merseyside, Proudman Oceanographic Laboratory, 92 p.
- Wöppelmann, G., Pouvreau, N., Simon, B., 2006. Brest sea level record: a time construction back to the early eighteenth century. *Ocean Dynamics* 56 (5–6), 487–497.